Published on *J. of Electromagnetic Waves and Appl.*, vol. 9, no. 1/2, pp. 71-83, January-February 1995 .

MOMENT METHOD SOLUTIONS USING PARAMETRIC GEOMETRY

J. M. Song and W. C. Chew
Electromagnetics Laboratory
Department of Electrical and Computer Engineering
University of Illinois
Urbana, IL 61801

Abstract

A technique for computing the electromagnetic (EM) radiation and scattering from three-dimensional (3D) conducting bodies of general shape is presented. The arbitrary surface is described by dividing it into a number of connected patches which are mathematically described as parametric quadratic surfaces. The electric field integral equation (EFIE) is discretized by the standard method of moments (MOM) with specially designed basis functions for subdomains which now contain surface curvature. The use of the basis functions on curvilinear patch reduces the number of unknowns used in MOM.

1. Introduction

Practical electromagnetic problems are often three-dimensional and involve arbitrary geometry. The scattering by arbitrary shaped conductors can be converted to finding the solution of an integral equation where the unknown function is the induced current distribution. The integral equation is discretized by the method of moments (MOM). There are three approaches to treat the geometry. The first approach is to approximate the geometry with thin-wire grids. Richmond [1] was the first to demonstrate the usefulness of this approach. The wire-grid model has been remarkably successful in those requiring the prediction of far-field quantities such as radiation patterns and radar cross section (RCS). However, this approach is not well suited for calculating near field and surface quantities such as surface current and input impedance. The second approach is to simulate the physical structure with flat surface patches. Several approaches to flat surface patch model have been reported in the literature, such as rectangular patches [2-4], triangular patches [5-6], and polygonal patches [7-8]. The flat surface patch model has been used to describe many simple and complicated objects, but it still creates unnecessary man-made discretization errors in the solution. Such errors become larger in the near field calculations. To obtain more accurate solution, more flat surface patches are needed.

The third approach to describe the arbitrary shape is to approximate the geometry with curved surface patches. Recently, many researchers have investigated the use of curved patches [9-15]. Knepp and Goldhirsh [9] divided an arbitrary surface into nonplanar quadrilateral patches and employed the magnetic field integral equation (MFIE) to solve the electromagnetic scattering problem with two pulse basis functions in each patch. Sancer, McClary, and Glover [10] solved MFIE and electric field integral equation (EFIE) using curvilinear patches with point matching and two pulse basis functions in each patch. Wilkes and Cha [11] extended the flat triangular patch moment method solution developed by Rao, Wilton, and Glisson [6] to the curved triangular patch. Wandzura [12] proposed a general and higher order current basis function for the curved triangular patch. Valle, Rivas, and Cátedra [13] recently solved EFIE by combining the moment method with geometrical modeling by NURBS surfaces and Bézier patches. One "roof-top" basis function is used at each pair of connected patches. More recently, Antilla and Alexopoulos [14] calculated the EM scattering from 3D geometries using a curvilinear hybrid finite-element-integral equation approach.

In this paper, a technique for computing the electromagnetic radiation and scattering from three dimensional conducting bodies with arbitrary shape is presented. The arbitrary surface is described by dividing it into a number of connected patches. Each is mathematically described as a parametric quadratic surface with fourth order polynomials (second order in each of two parameters). Thus, nine points on each patch must be well-known with respect to the origin of a known coordinate system. The electric field integral equation is discretized by standard MOM technique with specially designed basis functions for subdomains which now contain surface curvature. The basis functions are a generalization of "roof-top" functions [4]. The basis functions in [13] have a constant charge density in real space, and are expressed as an integral. Our basis functions have a constant charge density in parametric space, no line charge accumulation on each point of the common edge of adjacent cells, and are expressed in explicit form. The patch with larger electrical size is partitioned into a number of cells. Each pair of adjacent cells comprises one basis function. Also, patches which have a common edge are identified, and additional basis functions are required to allow a nonzero continuous current at patch-to-patch junctions. We use a number of basis functions on each patch and at the junctions of connected patches instead of one basis function in each pair of connected patches because the model is frequency independent, the number of basis functions but not the number of patches should increase as the frequency is increased.

2. Parametric Quadratic Surface Description

An arbitrary surface with curvature can generally be represented using two parameters: u_1 and u_2. The surface is then described by the equation $\mathbf{r}(u_1, u_2)$. A differential tangent vector is given by

$$d\mathbf{r} = \frac{\partial \mathbf{r}}{\partial u_1} du_1 + \frac{\partial \mathbf{r}}{\partial u_2} du_2. \tag{1}$$

Any vector tangential to the surface can be written as a linear combination of $\frac{\partial \mathbf{r}}{\partial u_1}$ and $\frac{\partial \mathbf{r}}{\partial u_2}$. Generally, the surface is composed of curvilinear patches. These patches are smoothly connected to each other at common boundaries. In this research, $\mathbf{r}(u_1, u_2)$ is a second-order polynomial in u_1 and u_2. Thus, nine points on each patch should be known with respect to the origin of a known coordinate system as shown in Figure 1. The locations of these nine points are then used to numerically generate the entire surface. The vector from the origin to the surface of the p-th patch may be written as

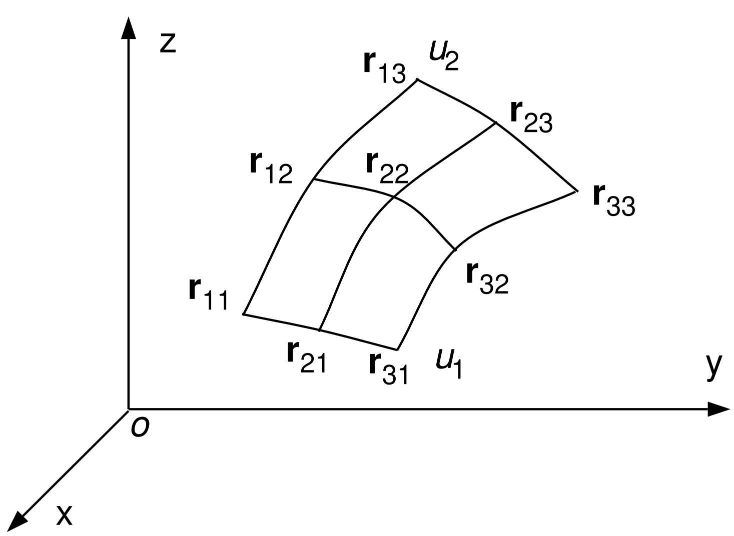

Figure 1. Curved quadrilateral patch defined by nine points.

$$\mathbf{r}_p(u_1, u_2) = \sum_{m=1}^{3} \sum_{n=1}^{3} \mathbf{C}_{mn}^{(p)} u_1^{m-1} u_2^{n-1} \tag{2}$$

for u_1 from 0 to 1, u_2 from 0 to 1, where $\mathbf{C}_{mn}^{(p)}$ are related to the known nine-point coordinates, and can be solved from the following linear equations

$$\begin{aligned}
\mathbf{r}_p(0,0) &= \mathbf{r}_{11} \\
\mathbf{r}_p(0,0.5) &= \mathbf{r}_{12} \\
\mathbf{r}_p(0,1) &= \mathbf{r}_{13} \\
\mathbf{r}_p(0.5,0) &= \mathbf{r}_{21} \\
\mathbf{r}_p(0.5,0.5) &= \mathbf{r}_{22} \\
\mathbf{r}_p(0.5,1) &= \mathbf{r}_{23} \\
\mathbf{r}_p(1,0) &= \mathbf{r}_{31} \\
\mathbf{r}_p(1,0.5) &= \mathbf{r}_{32} \\
\mathbf{r}_p(1,1) &= \mathbf{r}_{33}.
\end{aligned} \tag{3}$$

The distance between two nearby points parameterized by (u_1, u_2) and $(u_1 + du_1, u_2 + du_2)$ is given by

$$(ds)^2 = \sum_{i=1}^{2} \sum_{j=1}^{2} g_{ij}(u_1, u_2) du_1 du_2, \tag{4}$$

where

$$g_{ij} = \frac{\partial \mathbf{r}}{\partial u_i} \cdot \frac{\partial \mathbf{r}}{\partial u_j} \tag{5}$$

is known as the metric tensor. In differential geometry, it is often called the first principal form. The inverse of the metric tensor is its contravariant version g^{ij} [12]. The determinant of g_{ij} is

$$g = g_{11} g_{22} - g_{12}^2. \tag{6}$$

An oriented differential surface element is given by

$$d\mathbf{S} = \frac{\partial \mathbf{r}}{\partial u_1} \times \frac{\partial \mathbf{r}}{\partial u_2} du_1 du_2. \tag{7}$$

Using $(\mathbf{x} \times \mathbf{y})^2 = x^2 y^2 - (\mathbf{x} \cdot \mathbf{y})^2$, we have

$$dS = \sqrt{g} du_1 du_2. \tag{8}$$

Thus, the surface unit vector is

$$\widehat{n}(u_1, u_2) = \frac{1}{\sqrt{g}} \frac{\partial \mathbf{r}}{\partial u_1} \times \frac{\partial \mathbf{r}}{\partial u_2}. \tag{9}$$

The gradient of a scalar function on the surface, and the surface divergence of a vector function are given by

$$\nabla_S \phi = \sum_{i=1}^{2} \sum_{j=1}^{2} g^{ij} \frac{\partial \phi}{\partial u_i} \frac{\partial \mathbf{r}}{\partial u_j}, \tag{10}$$

and

$$\nabla_S \cdot \mathbf{f} = \sum_{i=1}^{2} \sum_{j=1}^{2} g^{ij} \frac{\partial \mathbf{f}}{\partial u_i} \cdot \frac{\partial \mathbf{r}}{\partial u_j} = \frac{1}{\sqrt{g}} \sum_{i=1}^{2} \frac{\partial (f_{u_i} \sqrt{g})}{\partial u_i}, \tag{11}$$

respectively, where

$$\mathbf{f} = f_{u_1} \frac{\partial \mathbf{r}}{\partial u_1} + f_{u_2} \frac{\partial \mathbf{r}}{\partial u_2}. \tag{12}$$

3. MOM Solutions and Basis Functions

For conducting objects, the EFIE is given by

$$\widehat{t} \cdot \int_S \left[\mathbf{J}(\mathbf{r}') + \frac{1}{k^2} \nabla' \cdot \mathbf{J}(\mathbf{r}') \nabla \right] \frac{e^{ikR}}{R} dS' = \frac{4\pi i}{k\eta} \widehat{t} \cdot \mathbf{E}^i(\mathbf{r}) \tag{13}$$

for $\mathbf{r}$ on surface S, where $\widehat{t}$ is any unit tangent vector on S, $\mathbf{E}^i$ is an impressed field which excites the system, and it is isolated in an impressed field region, or an incident plane wave, and $R = |\mathbf{r} - \mathbf{r}'|$.

The EFIE for the unknown electric current on the conducting surface induced by an incident wave is discretized using the method of moments (MOM) technique. The unknown current $\mathbf{J}(\mathbf{r})$ is first expanded in an appropriately chosen set of basis functions $\{\mathbf{j}_n\}$

$$\mathbf{J}(\mathbf{r}) = \sum_{n=1}^{N} a_n \mathbf{j}_n(\mathbf{r}), \tag{14}$$

where a_n are the unknown expansion coefficients. The EFIE for $\mathbf{J}(\mathbf{r})$ is discretized by substituting the above expansion in terms of unknowns a_n. Then, rather than forcing the EFIE to be satisfied for $\mathbf{r}$ on surface S, it is multiplied by a set of N testing functions $\{\mathbf{t}_m\}$ and the inner products are taken:

$$\sum_{n=1}^{N} A_{mn} a_n = F_m, \quad m = 1, 2, \cdots, N \tag{15}$$

where

$$A_{mn} = \int_S dS \mathbf{t}_m(\mathbf{r}) \cdot \int_S dS' \left[\mathbf{j}_n(\mathbf{r}') + \frac{1}{k^2} \nabla' \cdot \mathbf{j}_n(\mathbf{r}') \nabla \right] \frac{e^{ikR}}{R}, \tag{16}$$

$$F_m = \frac{4\pi i}{k\eta} \int_S dS \mathbf{t}_m(\mathbf{r}) \cdot \mathbf{E}^i(\mathbf{r}). \tag{17}$$

As shown in Figure 2(a), each patch is segmented into quadrilateral cells (in parametric space, these cells are rectangular) according the electrical size of curved surface, with a given maximum cell size in wavelengths. Each basis function comprises a pair of adjacent cells. The basis functions shown in Figure 2(b) are similar to the planar rooftop functions, and are given by

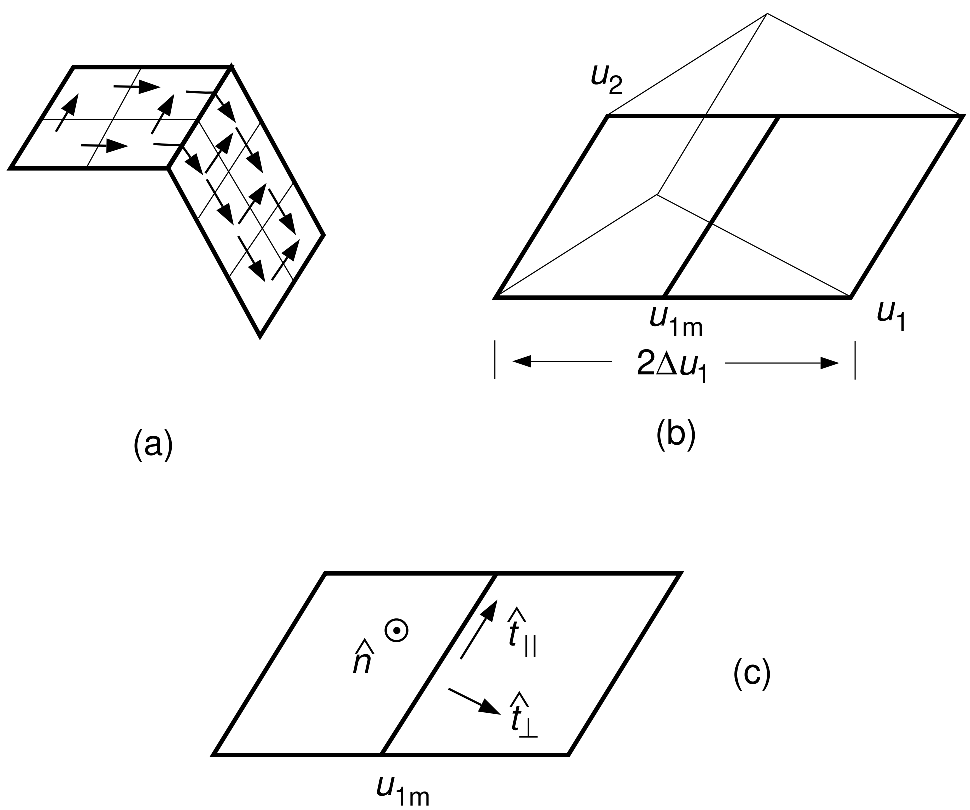

Figure 2. (a) Surface modes and overlap modes. (b) "Roof-top" basis function. (c) The normal component of the basis function on an edge.

$$\mathbf{j}_{u_{1m}} = \sqrt{\frac{g_{22}(u_{1m}, u_{2m})}{g(u_1, u_2)}} T_{u_{1m}}(u_1) P_{u_{2m}}(u_2) \frac{\partial \mathbf{r}}{\partial u_1} \tag{18}$$

along the $\frac{\partial \mathbf{r}}{\partial u_1}$ direction, and

$$\mathbf{j}_{u_{2m}} = \sqrt{\frac{g_{11}\left(u_{1m}, u_{2m}\right)}{g\left(u_1, u_2\right)}} T_{u_{2m}}\left(u_2\right) P_{u_{1m}}\left(u_1\right) \frac{\partial \mathbf{r}}{\partial u_2} \tag{19}$$

along the $\frac{\partial \mathbf{r}}{\partial u_2}$ direction. Here T_u is a triangular function which has the maximum value 1 on the common edge of the adjacent cells, and P_u is a pulse function.

Using Equations (11) and (18), we find the divergence of the basis functions

$$\nabla_S \cdot \mathbf{j}_{u_{1m}} = -\sqrt{\frac{g_{22}\left(u_{1m}, u_{2m}\right)}{g\left(u_1, u_2\right)}} \frac{\operatorname{sgn}(u_1 - u_{1m})}{\Delta u_1} W(u_1) P_{u_{2m}}\left(u_2\right), \tag{20}$$

where

$$W(u_1) = \begin{cases} 1, & (u_{1m} - \Delta u_1) < u_1 < (u_{1m} + \Delta u_1), \\ 0, & \text{otherwise.} \end{cases} \tag{21}$$

and

$$\operatorname{sgn}(u_1 - u_{1m}) = \begin{cases} 1, & u_1 > u_{1m}, \\ -1, & u_1 < u_{1m}. \end{cases} \tag{22}$$

The surface charge is found to be

$$\sigma dS = \frac{i}{\omega} \nabla_S \cdot \mathbf{j}_{u_{1m}} \sqrt{g(u_1, u_2)} du_1 du_2, \tag{23}$$

which is a constant in parametric space ($\frac{\sigma dS}{du_1 du_2}$). In real space, the charge density in the region with larger $\sqrt{g(u_1, u_2)}$ is less than that in the region with lesser $\sqrt{g(u_1, u_2)}$. This is in contrast to reference [13], where the basis functions are expressed in integral form, and have a constant charge density in the real space.

Next, we will find the normal component of the basis functions across the common edge ($u_1 = u_{1m}$). Referring to Figure 2(c), the unit tangent vector along u_1 isoparametric line is given by

$$\widehat{t}_{\parallel} = \frac{1}{\sqrt{g}_{22}} \frac{\partial \mathbf{r}}{\partial u_2}. \tag{24}$$

By taking the cross product between $\widehat{n}$ and $\widehat{t}_{\parallel}$, we find that the unit vector tangent to the surface and normal to the edge is

$$\widehat{t}_{\perp} = \widehat{t}_{\parallel} \times \widehat{n} = \frac{1}{\sqrt{g g_{22}}} [g_{22} \frac{\partial \mathbf{r}}{\partial u_1} - g_{12} \frac{\partial \mathbf{r}}{\partial u_2}]. \tag{25}$$

Using Equations (18) and (25), we find the normal component across the edge,

$$\widehat{t}_{\perp} \cdot \mathbf{j}_{u_{1m}} = \sqrt{\frac{g_{22}(u_{1m}, u_{2m})}{g_{22}(u_{1m}, u_2)}} P_{u_{2m}}(u_2). \tag{26}$$

The current density across the edge per unit parameter is independent of the geometry, because the denominator is just the differential length along this edge. Thus, there is no line charge accumulation on the common edge for the basis functions.

The basis functions for each surface patch are called surface modes. When two patches are connected, the additional basis functions called overlap modes [16] are required to allow a nonzero continuous current at patch-to-patch junctions. They are identical to the surface modes, except that each overlap mode belongs to two patches. Figure 2(a) shows two overlap modes at the junction of two patches. These overlap modes enforce the continuity of the normal component of current at the patch-to-patch junctions, and have a constant charge density in the parametric space.

Two kinds of testing functions are used. First, the testing functions are identical to the basis functions. This leads to a Galerkin's method. Second, we choose the testing functions as a constant along the line from the center of a cell to the center of an adjacent cell. We call it the "line matching" method. It is found that the line matching method has the same accuracy as the Galerkin's method. The numerical results presented in the next section are obtained using line matching method.

Once the basis and testing functions are found, the matrix elements A_{mn} in Equation (16) can be calculated. These double surface integrals in (16) are evaluated by three different ways depending on the distance between the basis function and the testing function. The first way is to numerically evaluate the surface integrals in the non-nearby terms using one to four point integration. The second way is to calculate the surface integrals in the nearby terms by Gaussian integration with more points. In the third way, the surface integrals in the self impedance terms are evaluated specially, since the Green's function contains an integrable singularity at $|\mathbf{r} - \mathbf{r}'|$. The procedure used to treat these singularities is to add and subtract a singular term from the integrals which can be integrated analytically and also renders the integrals well behaved so that standard numerical integration methods can be applied. The scalar potential integral can be written as

$$\int\int \frac{e^{ikR}}{R}\, du_1' du_2' = \int\int \left[\frac{e^{ikR}}{R} - \frac{1}{R_0}\right] du_1' du_2' + \int\int \frac{du_1' du_2'}{R_0}. \tag{27}$$

The function R_0, which should have the same behavior as near the singularity, is developed by using a Taylor series approximation of $\mathbf{r}'$ near $\mathbf{r}$. Thus R_0 is defined as

$$R_0 = \sqrt{g_{11}\left(u_1' - u_1\right)^2 + g_{22}\left(u_2' - u_2\right)^2 + 2g_{12}\left(u_1' - u_1\right)\left(u_2' - u_2\right)}, \tag{28}$$

where g_{11}, g_{22}, and g_{12} are evaluated at $\mathbf{r}$. Then the integral of $1/R_0$ can be found analytically,

$$\int_{u_{21}}^{u_{22}} \int_{u_{11}}^{u_{12}} \frac{du_1' du_2'}{R_0} = \left\{ \frac{u_1' - u_1}{\sqrt{g}_{22}} \ln\left[R_0 + \sqrt{g_{22}}(u_2' - u_2) + (u_1' - u_1)g_{12}/\sqrt{g_{22}}\right] \right.$$
$$\left. + \frac{u_2' - u_2}{\sqrt{g}_{11}} \ln\left[R_0 + \sqrt{g_{11}}(u_1' - u_1) + (u_2' - u_2)g_{12}/\sqrt{g_{11}}\right] \right\} \Bigg|_{u_1'=u_{11}}^{u_1'=u_{12}} \Bigg|_{u_2'=u_{21}}^{u_2'=u_{22}}. \tag{29}$$

4. Numerical Results

Numerical implementations are verified by comparing the results with some known ones in published papers for a conducting plate with different shapes. Figure 3 shows the computed current distribution on a circular disk illuminated by a normally incident plane wave. The component J_ϕ is shown along a diameter cut oriented perpendicular to the incident electric field vector. The disk is modeled by one curvilinear patch with eight points on the circle, and one point on the center. Also shown for comparison are the quasi-static solution valid at low frequencies [17], and the numerical solution by 56 triangular patches [6]. The agreement in Figure 3 is good.

The bistatic RCS in the H-plane for a conducting sphere with $ka = 0.5$ is shown in Figure 4. The sphere is modeled by six curvilinear patches with 48 unknowns. Also shown in the figure are the Mie series, the solution by 48 flat triangular patches with 72 unknowns, and by 40 Bézier patches with 76 unknowns [13]. It is seen that our results agree with the Mie series very well.

Figure 5 shows the RCS of the 14 inch long NASA almond at 2 GHz in the xy plane with $\theta = 90^o$. The almond is modeled by 13 curvilinear patches with 512 unknowns. 7 unknowns per wavelength are used. The results are compared to numerical results using flat polygonal patches with 655 piecewise sinusoidal basis functions and experimental measurements by Newman [16].

Sancer et al. [10] discussed the numerical breakdown of the EFIE at low frequencies. The breakdown is also present in the flat triangular patch code [18]. The RCS of a conducting sphere with one inch radius at different frequencies is shown in Table 1. It is found

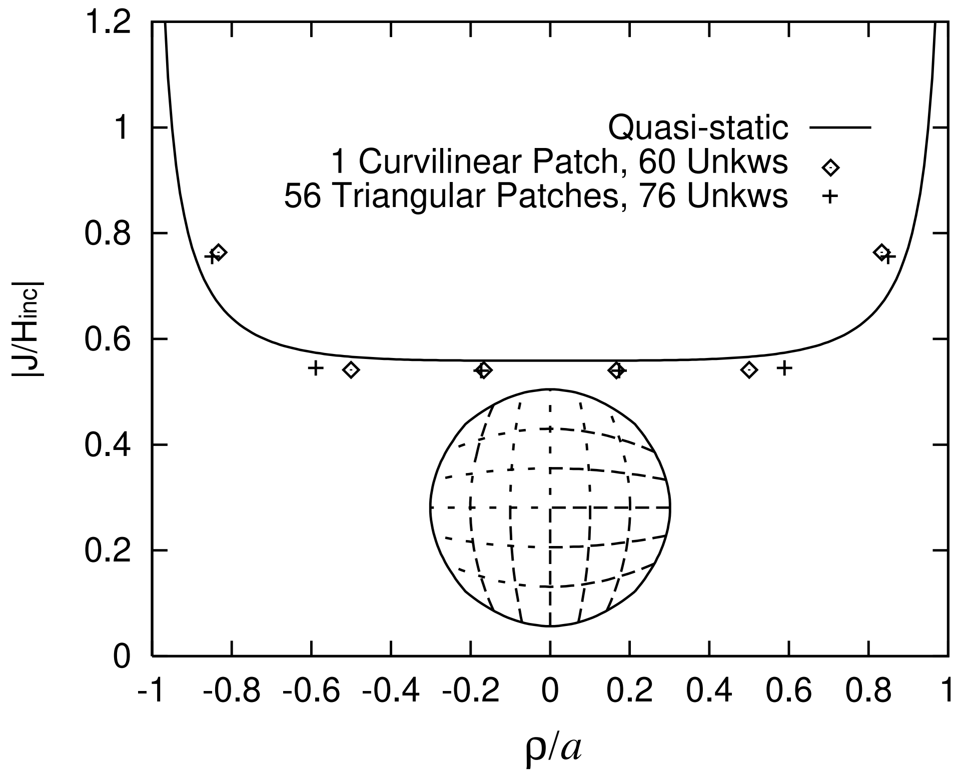

Figure 3. Comparison of the current distributions on 0.05 λ_0 radius circular disk calculated using one curvilinear patches with 60 unknowns, 56 triangular patches with 76 unknowns [6], and the quasi-static solution valid at low frequencies [17].

that the breakdown of our code is at 0.001 GHz ($ka = 0.00053$). It is lower than those by the flat triangular patch code (0.02 GHz, $ka = 0.01$), and by curvilinear patch code with pulse basis functions (0.5 GHz, $ka = 0.27$). The "roof-top" basis functions on the curvilinear patch give us a better result. Recently, Lim, Rao, and Wilton [19] defined a new pair of basis functions for flat triangular patch. These basis functions decompose the surface current density into divergence-less and curl-free parts which essentially decouple at the very low end of the frequency spectrum.

5. Conclusions

We have presented a technique for computing the electromagnetic radiation and scattering from 3D conducting bodies of arbitrary shape. The electric field integral equation is discretized by MOM with specially designed basis functions for subdomains which now contain surface curvature. The designed "roof-top" basis functions have a constant charge

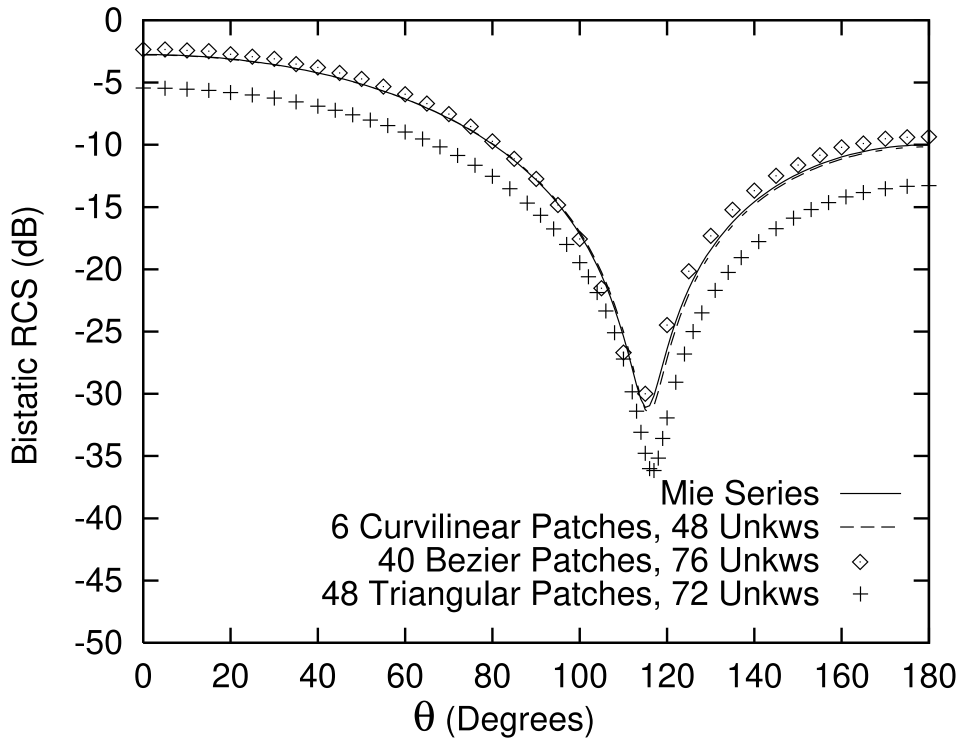

Figure 4. Bistatic RCS of a conducting sphere with $ka = 0.5$ calculated using 6 curvilinear patches with 48 unknowns, 48 flat triangular patches with 72 unknowns, 40 Bézier patches with 76 unknowns [13], and the Mie series. The RCS is normalized by πa^2.

density and no line charge accumulation on the surfaces. This approach needs fewer patches and unknowns, and has a lower breakdown frequency.

Acknowledgements

The authors would like to thank D.R. Wilton for pointing out some useful references for this work. This work was supported by NASA under grant NASA NAG 2-871, Office of Naval Research under grant N00014-89-J1286, the Army Research Office under contract DAAL03-91-G-0339, and the National Science Foundation under grant NSF ECS 92-24466.

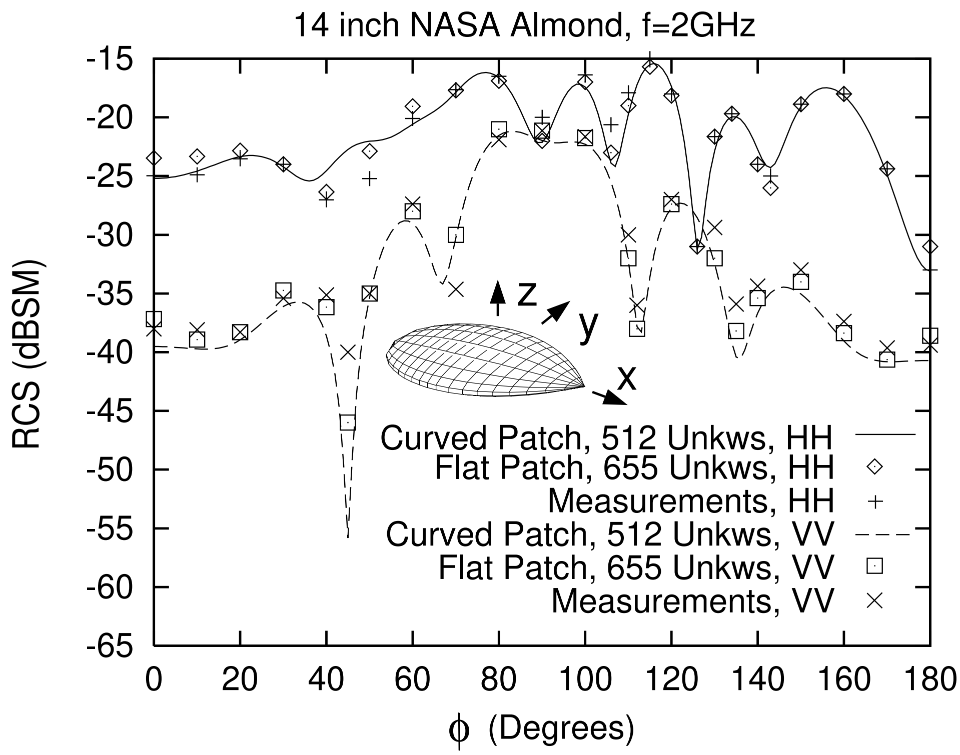

Figure 5. RCS of a 14 inch long NASA almond at 2 GHz in the xy plane with $\theta = 90^o$. The numerical results and experimental measurements by Newman [16] are also given for comparison.

Table 1. Differences in dB between the Mie series and numerical results for a conducting sphere with one inch radius

Frequency (GHz)	Quadrilateral Curved Patch "Roof-top" basis (320 unknowns)	Triangular Flat Patch [10] (336 unknowns)	Quadrilateral Curved Patch Pulse Basis [10] (338 unknowns)
0.001	21.66		
0.002	0.555	-4.15	-3.38
0.005	0.361	-4.77	-3.39
0.010	-0.087	0.27	-3.39
0.020	-0.039	19.29	-3.39
0.050	-0.032	-0.29	-3.44
0.200	-0.030	-0.66	-4.63
0.500	-0.030	-0.67	5.59
1.000	-0.031	-0.67	0.66
1.500	-0.025	-0.57	0.39
2.000	-0.007	-0.28	0.34

References

[1] J.H. Richmond, "A Wire-grid Model for Scattering by Conducting Bodies," *IEEE Trans. Antennas Propagat.*, vol. 14, no. 6, pp. 782-786, Nov. 1966.

[2] N.N. Wang, J.H. Richmond, and M.C. Gilreath, "Sinusoidal Reaction Formulation for Radiation and Scattering from Conducting Surfaces," *IEEE Trans. Antennas Propagat.*, vol. 23, no. 3, pp. 376-382, May 1975.

[3] E.H. Newman and D.M. Pozar, "Electromagnetic Modeling of Composite Wire and Surface Geometries," *IEEE Trans. Antennas Propagat.*, vol. 26, no. 6, pp. 784-789, Nov. 1978.

[4] A.W. Glisson and D.R. Wilton, "Simple and Efficient Numerical Methods for Problems of Electromagnetic Radiation and Scattering from Surfaces," *IEEE Trans. Antennas Propagat.*, vol. 28, no. 5, pp. 593-603, Sept. 1980.

[5] J.J.H. Wang, "Numerical Analysis of Three-dimensional Arbitrarily-shaped Conducting Scatters by Trilateral Surface Cell Modeling," *Radio Sci.*, vol. 13, no. 6, pp. 947-952, Nov.-Dec. 1978.

[6] S.M. Rao, D.R. Wilton, and A.W. Glisson, "Electromagnetic Scattering by Surfaces of Arbitrary Shape," *IEEE Trans. Antennas and Propagat.*, vol. 30, no. 3, pp. 409-418, May 1982.

[7] E.H. Newman and P. Tulyatha, "A Surface Patch Model for Polygonal Plates," *IEEE Trans. Antennas Propagat.*, vol. 30, no. 4, pp. 588-593, July 1982.

[8] E.H. Newman, P. Alexandroupoulos, and E.K. Walton, "Polygonal Plate Modeling of Realistic Structures," *IEEE Trans. Antennas Propagat.*, vol. 32, no. 7, pp. 742-747, July 1984.

[9] D.L. Knepp and J. Goldhirsh, "Numerical Analysis of Electromagnetic Radiation Properties of Smooth Conducting Bodies of Arbitrary Shape," *IEEE Trans. Antennas Propagat.*, vol. 20, no. 3, pp. 383-388, May 1972.

[10] M.I. Sancer, R.L. McClary, and K.J. Glover, "Electromagnetic Computation Using Parametric Geometry," *Electromagnetics*, vol. 10, no. 1-2, pp. 85-103, 1990.

[11] D.L. Wilkes and C.-C. Cha, "Method of Moments Solution with Parametric Curved Triangular Patches," *1991 International IEEE AP-S Symposium Digest*, pp. 1512-1515, London, Ontario, Canada, 1991.

[12] S. Wandzura, "Electric Current Basis Functions for Curved Surfaces," *Electromagnetics*, vol. 12, pp. 77-91, 1992.

[13] L. Valle, F. Rivas, and M.F.Cátedra, "Combining the Moment Method with Geometrical Modeling by NURBS Surfaces and Bézier Patches," *IEEE Trans. Antennas and Propagat.*, vol. 42, no. 3, pp. 373-381, March 1994.

[14] G.E. Antilla and N.G. Alexopoulos, "Scattering from Complex Three-dimensional Geometries Using a Curvilinear Hybrid Finite-element-integral Equation Approach," *J. Optical Soc. America A*, vol. 11, no. 4, pp. 1445-1457, April 1994.

[15] J.M. Song and W.C. Chew, "Moment Method Solution Using Parametric Geometry," *1994 International IEEE AP-S Symposium Digest*, vol. 3, pp.2242-2245, Seattle, Washington, June 1994.

[16] E.H. Newman, "Polygonal Plate Modeling," *Electromagnetics*, vol. 10, no. 1-2, pp. 65-83, 1990.

[17] J.J. Bowman, T.B.A. Senior, and P.L.E. Uslenghi, *Electromagnetic and Acoustic Scattering by Simple Shapes*, Amsterdam: North-Holland, 1969, pp. 576-577.

[18] W.A. Johnson, D.R. Wilton, and R.M. Sharpe, "Modeling Scattering from and Radiation by Arbitrary Shaped Objects with the Electric Field Integral Equation Triangular Surface Patch Code," *Electromagnetics*, vol.10, no. 1-2, pp. 41-63, 1990.

[19] J.S. Lim, S.M. Rao, and D.R. Wilton, "A Novel Technique to Calculate the Electromagnetic Scattering by Surfaces of Arbitrary Shape," *Digest of the 1993 URSI Radio Science Meeting*, p. 322, Ann Arbor, Michigan, June 1993.

Jiming Song received the B.S. and M.S. degrees, both in Physics, from Nanjing University, China, in 1983 and 1988, respectively, and Ph.D. degree in Electrical Engineering from Michigan State University in 1993. From 1983 to 1985, he worked in the Microwave Engineering Department of Beijing Broadcasting College. His current interests focus on the wave scattering using fast algorithm, the wave interaction with inhomogeneous media. He is currently a visiting research associate at the University of Illinois. He is a member of Phi Kappa Phi and was the recipient of the Outstanding Academic Award from the College of Engineering, Michigan State University, in 1992.

Weng Cho Chew received the B.S. degree in 1976, both the M.S. and Engineer's degrees in 1978, and the Ph. D. degree in 1980, all in electrical engineering from the Massachusetts Institute of Technology, Cambridge, MA.

His research interest is in the area of waves in inhomogeneous media for various sensing applications, integrated circuits, microstrip antenna applications, and fast algorithms for solving wave scattering problems. He is now a professor at the University of Illinois. Before coming to University of Illinois, he was a department manager at Schlumberger-Doll Research. He is an IEEE Fellow, and was an NSF Presidential Young Investigator and has been active with various journals and societies. He has authored a book entitled "Waves and Fields in Inhomogeneous Media"